Post-ablation evolution of the tungsten VUV/XUV spectra in JET

E. Pawelec[1], S. S. Henderson[2], M. G. O'Mullane[2], E. R. Solano[3], A. Huber[4], A. Baciero[3], J. Boom[5], I. Coffey[6], J. Flanagan[5], S. Jachmich[4], K. Lawson[5], M. Maslov[2], L. Meneses[7], S. Menmuir[5], T. Pütterich[8], S. Schmuck[5], G. Sergienko[3], M. Stamp[5], H. P. Summers[2] and JET Contributors*

[1]Institute of Physics, Opole University, Oleska 48, 45-052 Opole, Poland; [2]Department of Physics, University of Strathclyde, Glasgow G4 0NG, UK; [3]Laboratorio Nacional de Fusión, CIEMAT, Avda Complutense 40, 280040 Madrid, Spain; [4]Forschungszentrum Jülich GmbH, 52425 Jülich, Germany; [5]UKAEA-EURATOM Association, Culham Science Centre, Abingdon, OX14 3DB, UK; [6]Queens University Belfast, BT71NN, UK; [7]Instituto de Plasmas e Fusao Nuclear, Universidade de Lisboa, Portugal; [8]Max-Planck-Institut für Plasmaphysik, D-85748 Garching, Germany

We posit that the introduction of tungsten into fusion plasmas significantly changes their behaviour due to considerable cooling of the pedestal. Study of this hypothesis depends on understanding both the transport of tungsten in the fusion plasma and its radiative properties. Most of the tungsten radiation in the $T_e < 2$ keV temperature range emits in the VUV and XUV regions, where many close-lying lines from different ionization stages form broad spectroscopic features. Analysis of such features is challenging [1], especially when the studied spectra are composed of contributions from different temperature regions in addition to the overlapping ionization stages. Some simplification is possible by modelling the emission from single ions produced in electron-beam ion traps, where these EBIT spectra are used to validate the atomic model which is then applied to the tokamak spectrum [2].

The presence of sawteeth can dominate the transport and introduce non-local T_e effects [3], so in this experiment tungsten is ablated into JET L-mode, low temperature ($T_e < 2$ keV), non-sawtoothing plasmas. The ablation is in the ramp-up phase of the pulse (at 3.1s) with magnetic field of B = 3T, current Ip = 1.55 MA at the moment of ablation rising to 1.7 MA from 3.5s. The pulse is heated by 1 MW neutral beam additional power and Z_{eff} is ~1.3 which does not change visibly during the evolution of the tungsten emission following the ablation.

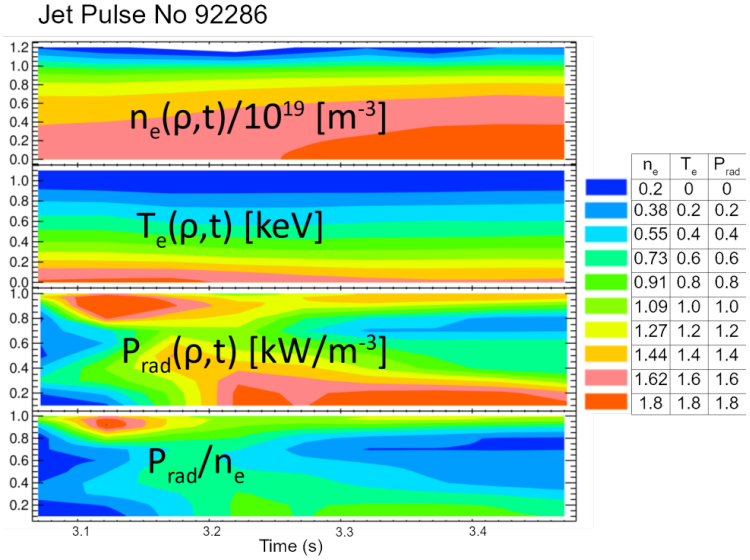

Fig 1. Evolution of the plasma parameter profiles during the studied phases of the ablation experiment. Note that P_{rad}/n_e is proportional to the cooling factor, $n_W L_W(T_e)$, and shows the penetration of tungsten to the plasma core.

*See the author list of Litaudon et al, "Overview of the JET results in support to ITER", accepted for publication in Nuclear Fusion.

After the ablation the plasma radiated power sharply rises, but most of the radiation is localized at the outer ring (figures 1, 2). Radiation originating from the centre of the plasma rises much more slowly and reaches a maximum after approximately 100ms. This moment can be considered as the time point from which the horizontal and vertical lines of sight of the observing spectrometers (see figure 3) intersect the same region of the radiating tungsten cloud and when most of the radiation registered by bolometer cameras is emitted by tungsten. During this period the plasma parameters change slowly, by ~10% of their initial values: the electron density increases and the temperature decreases, both in the plasma core and in the plasma edge.

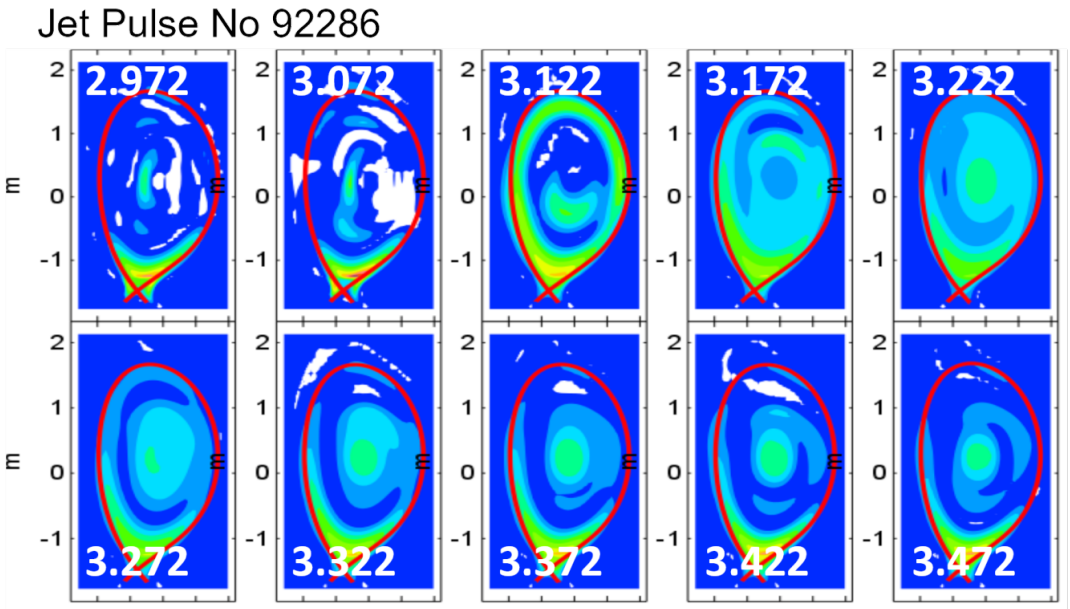

Fig 2. Bolometry results before and after ablation, averaged over 50 ms time frames. The ablation is at 3.1s.

Figure 2 shows a reconstruction of the radiated power from the bolometer. Just after the ablation, the radiation is localised along the separatrix; this radiation is from not only tungsten, but also lighter species, mostly deuterium. After 70-100ms the radiation maximum shifts to the plasma core and thereafter its intensity starts to slowly decrease, with the temporal dependence nearly the same as for the plasma parameters.

A synthetic diagnostic measure of the tungsten radiation, corresponding to a mid-plane bolometer line-of-sight (LoS) view, as shown by the red line in figure 3a, is modelled using the interpretative code JETTO [4]. Theoretical modelling of the tungsten transport suggests anomalous diffusive transport in the plasma core and a neoclassical convection near the plasma edge. In these conditions, the temporal evolution of the line-integrated radiation along a single LoS is most sensitive to the choice of plasma transport coefficients, whereas the radiation profile across the plasma radius is mainly dependent on the choice of the input atomic data. Tungsten transport coefficients used in this analysis are shown in figure 3b as a function of $\rho=\sqrt{\varphi_N}$ and are simplified such that they are fixed in both time and in charge. The temporal evolution of the synthetic radiation along the mid-plane LoS in compared to the bolometer measurement in figure 3c.

The profile of the measured radiated power normalized to the electron density (P_{rad}/n_e or $n_W L_W$, where n_W is the tungsten concentration and Lw(Te) is the cooling function), extracted from the inverted bolometry reconstruction at t=3.37s is shown as a function of ρ by the dashed-dot line in figure 3d. The equivalent synthetic prediction is shown for two different sets of atomic

data: (i) a baseline set corresponding to ionisation, recombination, and total line power coefficients from the Asdex Upgrade studies [1] and (ii) a modified set based on (i) but with new line power coefficients [5] and adjusted dielectronic recombination rates for tungsten ions with open *4f* shells (W^{15+} – W^{27+}). The alteration of the DR rate is to account for an enhancement factor seen in these stages in storage ring measurements [6]. The Te profile is shown for reference in figure 3e. The drop in P_{rad}/n_e between ρ=0.2-0.4 suggests that L_W is falling more sharply as Te decreases from 1.3–1.0keV, whereas the flatter P_{rad}/n_e measurement between ρ=0.4–0.6 indicates either a flat or increasing cooling function L_W as T_e decreases from 1.0–0.6keV. The baseline data does not recover either feature whereas the enhanced baseline data better reproduces the flatter P_{rad}/n_e.

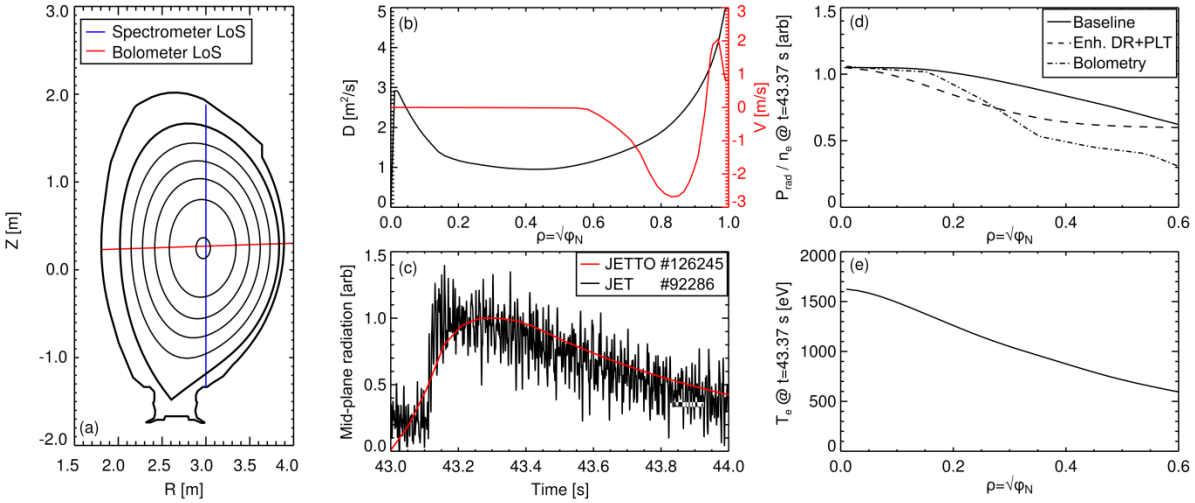

Fig 3. The spectrometer (blue) and bolometer (red) line-of-sight (LoS) used for synthetic diagnostic measurements are shown in (a). Tungsten transport coefficients used in JETTO are shown in (b). A comparison of the synthetic and experiment radiation along the bolometer LoS is given in (c). The measured P_{rad}/n_e from inverted bolometry measurements at t=43.37 s is shown by the dashed-dot line in (d) along with the synthetic measurement based on two different sets of atomic data (see text). The temperature profile is shown for reference in (e).

As tungsten penetrates the plasma from its initial ablation point at the outer mid-plane, we observe changes in both its spatial distribution and in the shape of the spectral features observed by different spectrometers. There are four spectrometers used:

- two VUV (15–140 nm and 14–45 nm) and one XUV (4–7 nm) spectrometers with vertical line of sight through the plasma centre, and
- one VUV spectrometer (10–104 nm) with horizontal line of sight slightly below the plasma centre, collinear with the insertion port of ablation material.

The VUV spectra presented in figure 4 are restricted to the 10–45 nm wavelength region, as tungsten features for longer wavelengths are very weak. An average of five frames before the ablation is subtracted from the spectrum presented, to restrict the spectrum only to the features introduced with ablated tungsten. It can be seen, that just after ablation the spectrum observed along the horizontal LoS is different from the one observed along the vertical LoS, but after 50 ms the spectra from different directions have very similar shape and from 100 ms even the ratio of their amplitudes is nearly constant. This is consistent with the assumption, that the vertical (excluding divertor region) and horizontal temperature and W density profiles 100 ms after ablation are very similar. VUV features appear at the moment of ablation and decay relatively quickly, with characteristic times from 160 to 200 ms. The XUV feature between 4 and 7 nm increases much more slowly, reaching the maximum at the same moment as when the bolometry shows the maximum radiation in the plasma core and its characteristic time of

decay is the same as for the total radiation, 470 ms. It can be seen, that the shape of both VUV and XUV spectrum change slightly during the decay, which most probably reflects changes in temperature of the radiating tungsten population.

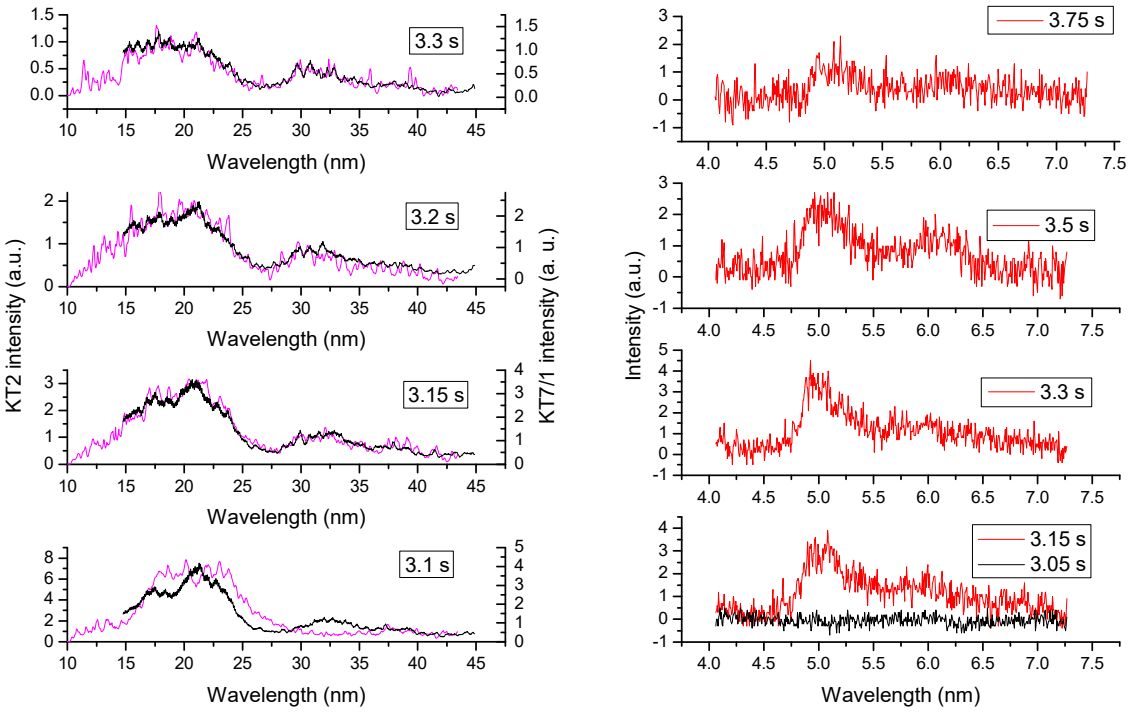

Fig 4. Temporal evolution of VUV and XUV spectra. Left – VUV spectra from vertical (black) and horizontal (magenta) line of sight. Wavelength dependent calibration sensitivities have been applied to each spectrometer. Right – XUV spectra from vertical line of sight. The sensitivity response is expected to be flat as a function of wavelength for this instrument.

The spectral feature from 10–45 nm is driven by emission from tungsten ions ranging from Z=16–30. Furthermore, this emission is mainly driven by the $4f^n\ 5p - 4f^n\ 5s$ transition, where n is the number of electrons specific for each ion. However, since the total power is driven mainly by transitions involving the open *4d* shell, this weaker emission feature is mainly a result of electron excitation and de-excitation flow within the ion and is therefore particularly sensitive to the population modelling and the configurations included in the fundamental atomic modelling codes. Efforts have been made in the past to try and model this spectral feature using emission from ions Z=23–26 [1,7], however only emission from Z=23 has been treated in with an extensive configuration set. Including all relevant configurations for each of ions in this charge range generally results in calculations exceeding computational limits, especially for the ions of charge Z=18–22. As a future step, an attempt will be made to try and model the emission emanating from Z=23–26 coupled with an ionisation balance to try and assess this feature.

This work has been carried out within the framework of the EUROfusion Consortium and has received funding from the Euratom research and training programme 2014-2018 under grant agreement No 633053. The views and opinions expressed herein do not necessarily reflect those of the European Commission.

[1] T. Pütterich et al, Plasma Physics and Controlled Fusion **50**, 085016 (2008); [2] H. A. Sakaue et al, Physical Review A **92**, 012504, (2015) [3] E. R. Solano et al, 43rd EPS Conference on Plasma Physics, P2.005 (2016); [4] G. Cenacchi and A. Taroni, Rapporto ENEA RT/TIB 88(5), (1988); [5] S. Henderson et al., Plasma Physics and Controlled Fusion **59,** 055010 (2017); [6] N R Badnell et al, Phys. Rev. A, **85**, 052716 (2012); [7] T. Pütterich et al, AIP Conf. Proc. **1545**, 132 (2013),